SUPPLEMENTARY INFORMATION

New multicomponent catalysts for the selective aerobic oxidative condensation of benzylamines to N-benzylidenbenzylamine

Cristina Madalina Opris,[a] Octavian Pavel,[a] Alaina Moragues,[b] Jamal El Haskouri,[b,c] Daniel Beltrán,[b] Pedro Amorós,[b*] M. Dolores Marcos,[d] Laura Elena Stoflea,[e] Vasile I. Parvulescu[a*]

[a] University of Bucharest, Department of Organic Chemistry and Catalysis, Bdul Regina Elisabeta 4-12, 030016 Bucharest, Romania, vasile.parvulescu@g.unibuc.ro
[b] Institut de Ciencia dels Material, Universitat de Valencia, P. O. Box 22085, Valencia E46071, Spain, pedro.amoros@uv.es
[c] Fundació General, Universitat de València. P. O. Box 22085, 46071-Valencia, Spain
[d] Centro de Reconocimiento Molecular y Desarrollo Tecnológico (IDM), Departamento de Química, Universidad Politécnica de Valencia, Camino de Vera s/n, 46022-Valencia, Spain
[e] National Institute of Materials Physics, PO Box MG-07, 077125 Bucharest-Magurele, Romania

Catalysts characterization

Figures S1 and S2 show the high-angle XRD patterns of all synthesized UVM-7-based materials, after and before the gold incorporation and thermally processed at 200 and 500ºC.

Figures S3 and S4 correspond to TEM images and N_2 adsorption-desorption isotherms of the gold-free support/catalysts. The nickel inclusion does not affect the mesostructure when compared with a TEM image of UVM-7 pure silica. The two pore systems (intraparticle surfactant generated mesopore system and the interparticle disordered large pores) result clearly appreciated. The Ce and Sn inclusion although does not affect in a qualitative way the original mesostructure, the incorporation of these heteroelements favors a certain interparticle condensation with the subsequent relatively loss of textural-type porosity.

Cristina Madalina Opris,[a] Octavian Pavel,[a] Alaina Moragues,[b] Jamal El Haskouri,[b,c] Daniel Beltrán,[b] Pedro Amorós,[b*] M. Dolores Marcos,[d] Laura Elena Stoflea,[e] Vasile I. Parvulescu[a*]

[a] University of Bucharest, Department of Organic Chemistry and Catalysis, Bdul Regina Elisabeta 4-12, 030016 Bucharest, Romania, vasile.parvulescu@g.unibuc.ro
[b] Institut de Ciencia dels Material, Universitat de Valencia, P. O. Box 22085, Valencia E46071, Spain, pedro.amoros@uv.es
[c] Fundació General, Universitat de València. P. O. Box 22085, 46071-Valencia, Spain
[d] Centro de Reconocimiento Molecular y Desarrollo Tecnológico (IDM), Departamento de Química, Universidad Politécnica de Valencia, Camino de Vera s/n, 46022-Valencia, Spain
[e] National Institute of Materials Physics, PO Box MG-07, 077125 Bucharest-Magurele, Romania

Catalysts characterization

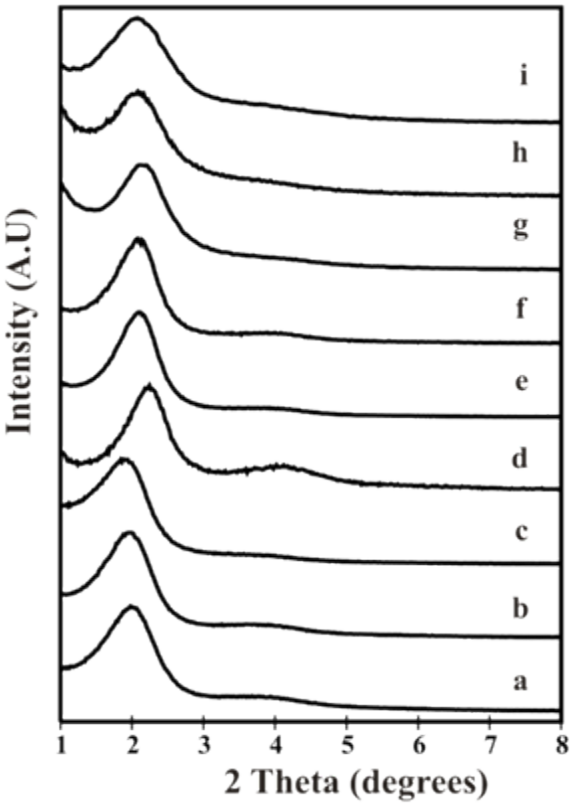

Fig. SI1. Low-angle XRD patterns of the gold-free supports. (a) Ni60-UVM-7, (b) Ni30-UVM-7, (c) Ni10-UVM-7, (d) Ce_{60}-Ni_{10}-UVM-7, (e) Ce_{30}-Ni_{10}-UVM-7, (f) Ce_{10}-Ni_{10}-UVM-7, (g) Sn_{60}-Ni_{10}-UVM-7, (h) Sn_{30}-Ni_{10}-UVM-7 and (i) Sn_{10}-Ni_{10}-UVM-7.

Figures SI2 and SI3 show the high-angle XRD patterns of all synthesized UVM-7-based materials, after and before the gold incorporation and thermally processed at 200 and 500ºC.

Figures SI4 and SI5 correspond to TEM images and N_2 adsorption-desorption isotherms of the gold-free support/catalysts. The nickel inclusion does not affect the mesostructure when compared with a TEM image of UVM-7 pure silica. The two pore systems (intraparticle surfactant generated mesopore system and the interparticle disordered large pores) result clearly appreciated. The Ce and Sn inclusion although does not affect in a qualitative way the original mesostructure, the incorporation of these heteroelements favors a certain interparticle condensation with the subsequent relatively loss of textural-type porosity.

Figs. SI5 and SI6 present N_2 adsorption desorption isotherms of catalysts : **SI5** (a) Au/Sn_{10}-Ni_{10}-UVM-7, (b) Au/Sn_{30}-Ni_{10}-UVM-7 and (c) Au/Sn_{60}-Ni_{10}-UVM-7, processed at (i) 200ºC and (ii) 500ºC. **SI6** (a) Au/Ce_{10}-Ni_{10}-UVM-7, (b) Au/Ce_{30}-Ni_{10}-UVM-7 and (c) Au/Ce_{60}-Ni_{10}-UVM-7, processed at (i) 200ºC and (ii) 500ºC

Figs. SI7 and SI8 present the BJH pore size distributions from the adsorption branches of the N_2 adsorption-desorption isotherms of catalysts: **SI7** (a) Au/Ce_{10}-Ni_{10}-UVM-7, (b) Au/Ce_{30}-Ni_{10}-UVM-7 and (c) Au/Ce_{60}-Ni_{10}-UVM-7, processed at (i) 200ºC and (ii) 500ºC. **SI8**. (a) Au/Sn_{10}-Ni_{10}-UVM-7, (b) Au/Sn_{30}-Ni_{10}-UVM-7 and (c) Au/Sn_{60}-Ni_{10}-UVM-7, processed at (i) 200ºC and (ii) 500ºC.

Figs. SI9 and SI10 present conversion results in recycling experiments

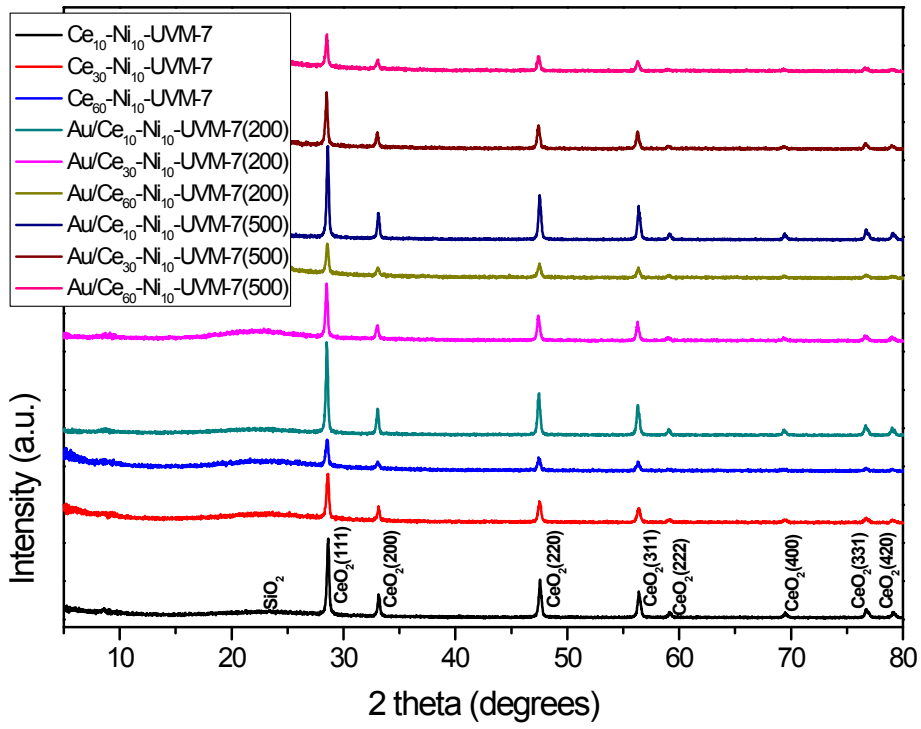

Fig. SI2. High-angle XRD patterns of the supports and final catalysts containing Ce.

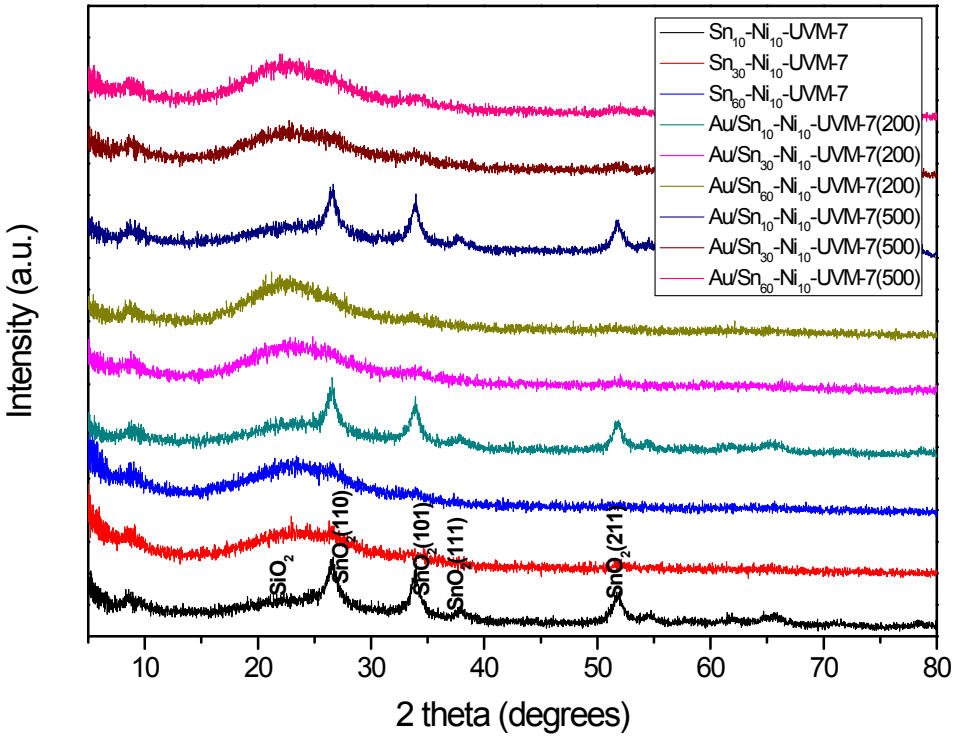

Fig. SI3. High-angle XRD patterns of the supports and final catalysts containing Sn.

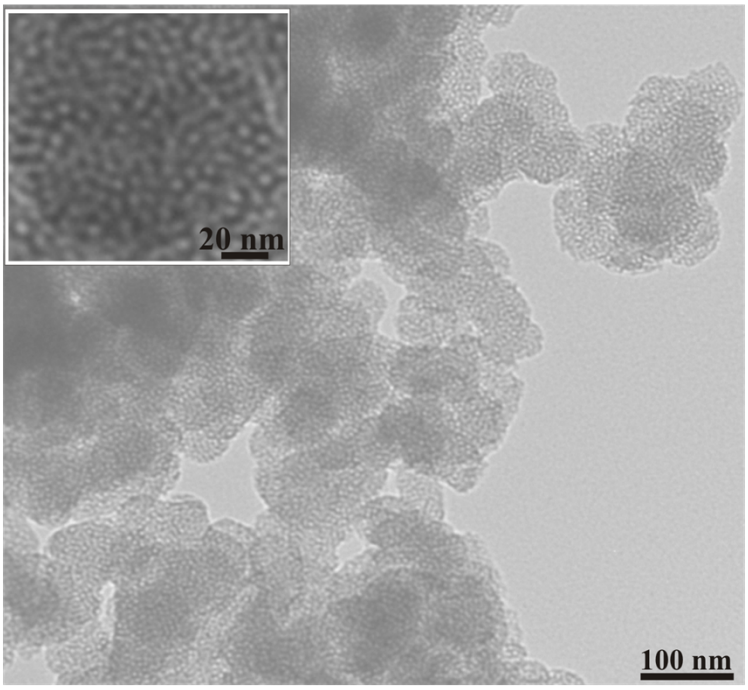

Fig. SI4. Representative TEM image of Ni_x-UVM-7 samples (x=10).

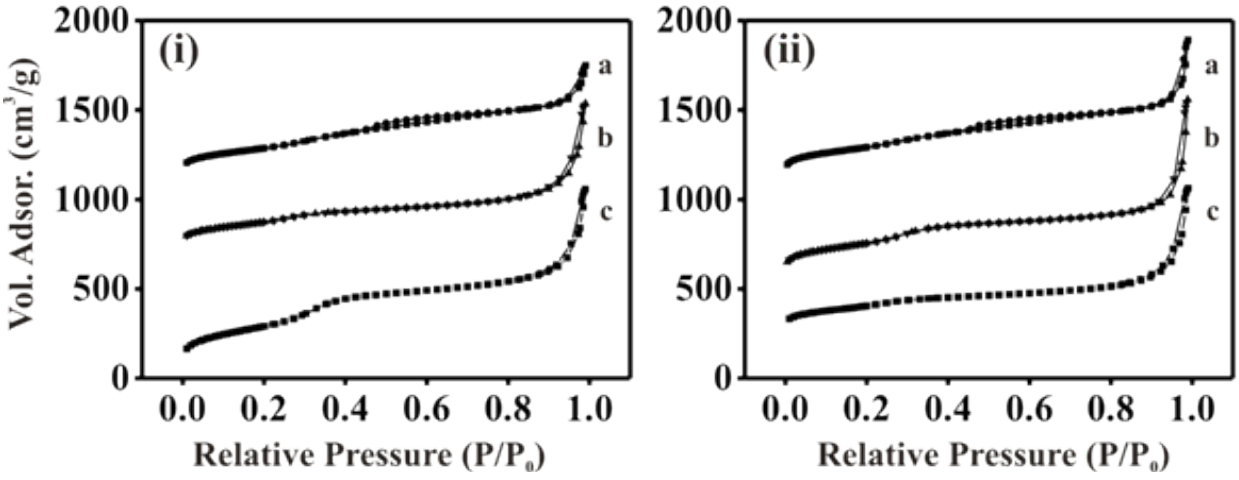

Fig. SI5. N_2 adsorption desorption isotherms of catalysts (a) Au/Sn_{10}-Ni_{10}-UVM-7, (b) Au/Sn_{30}-Ni_{10}-UVM-7 and (c) Au/Sn_{60}-Ni_{10}-UVM-7, processed at (i) 200ºC and (ii) 500ºC.

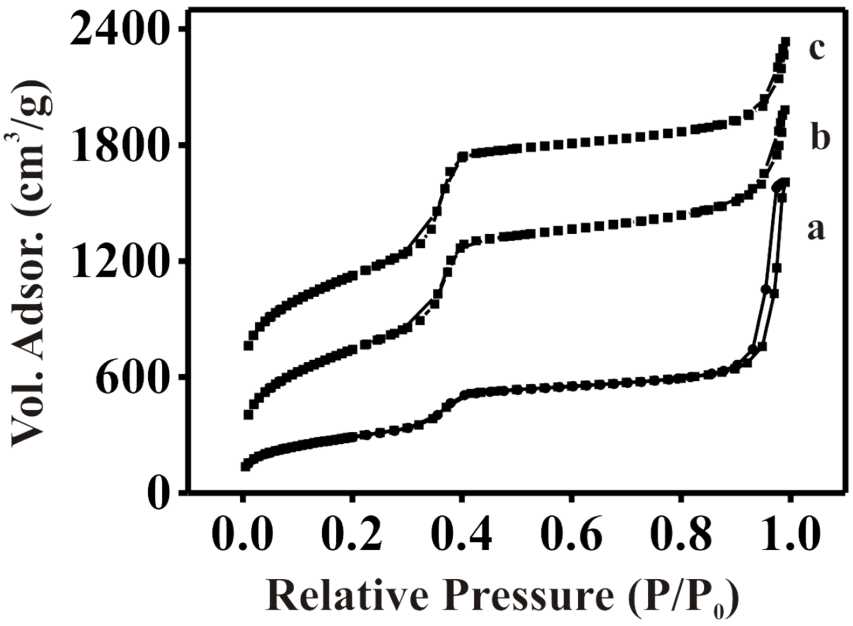

Fig. SI6. Representative N_2 adsorption-desorption isotherms of the gold-free supports. (a) Ni_{60}-UVM-7, (b) Ce_{60}-Ni_{10}-UVM-7 and (c) Sn_{60}-Ni_{10}-UVM-7.

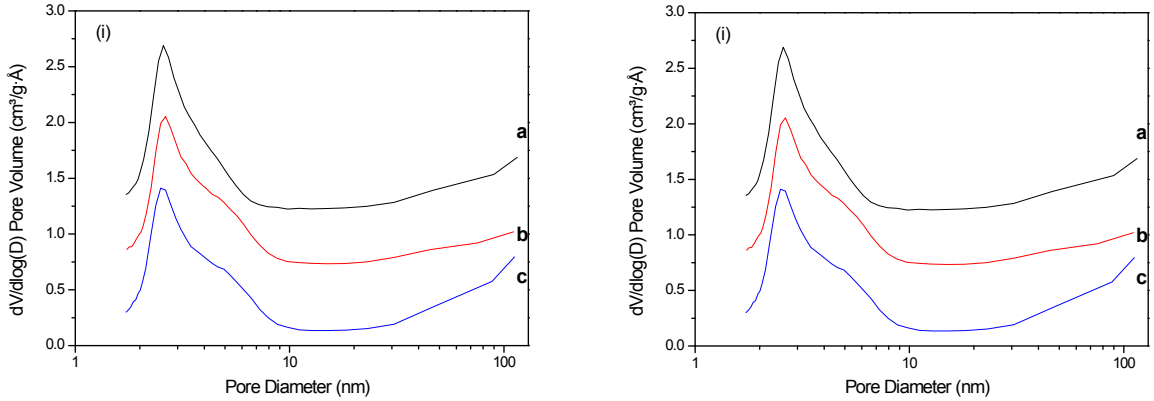

Fig. SI7. BJH pore size distributions from the adsorption branches of the N_2 adsorption-desorption isotherms of catalysts (a) Au/Ce_{10}-Ni_{10}-UVM-7, (b) Au/Ce_{30}-Ni_{10}-UVM-7 and (c) Au/Ce_{60}-Ni_{10}-UVM-7, processed at (i) 200ºC and (ii) 500ºC.

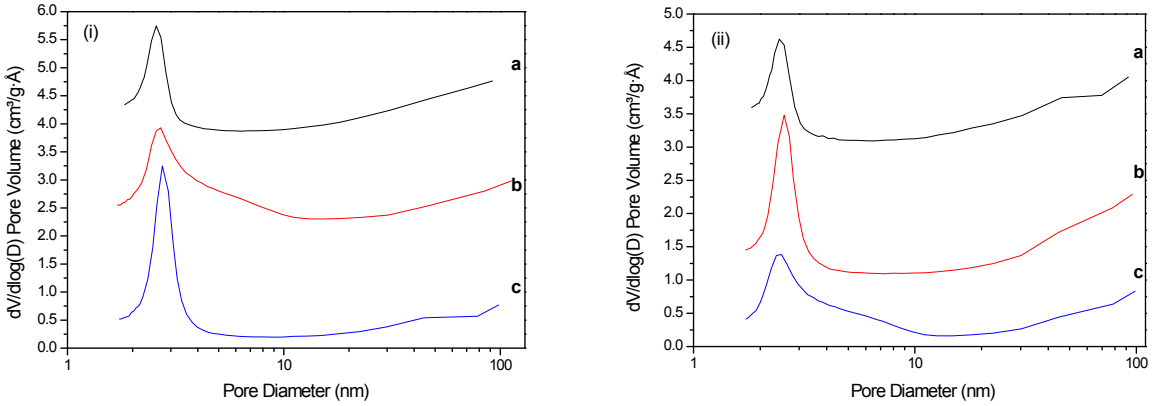

Fig. SI8. BJH pore size distributions from the adsorption branches of the N_2 adsorption desorption isotherms of catalysts (a) Au/Sn_{10}-Ni_{10}-UVM-7, (b) Au/Sn_{30}-Ni_{10}-UVM-7 and (c) Au/Sn_{60}-Ni_{10}-UVM-7, processed at (i) 200ºC and (ii) 500ºC.

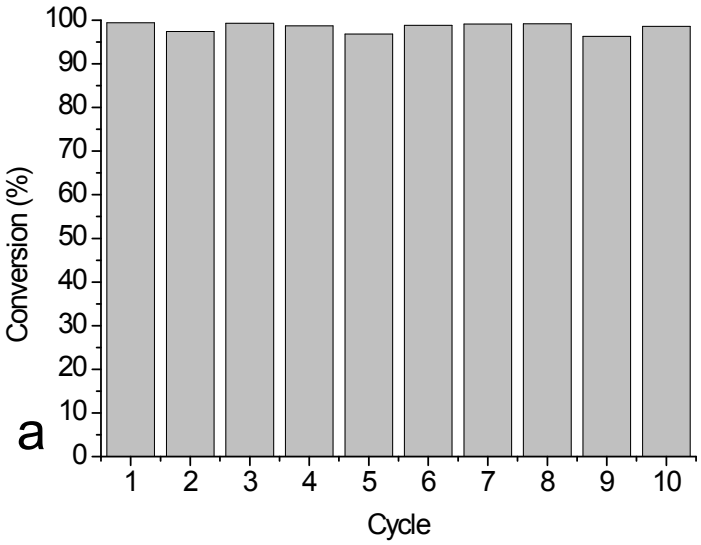

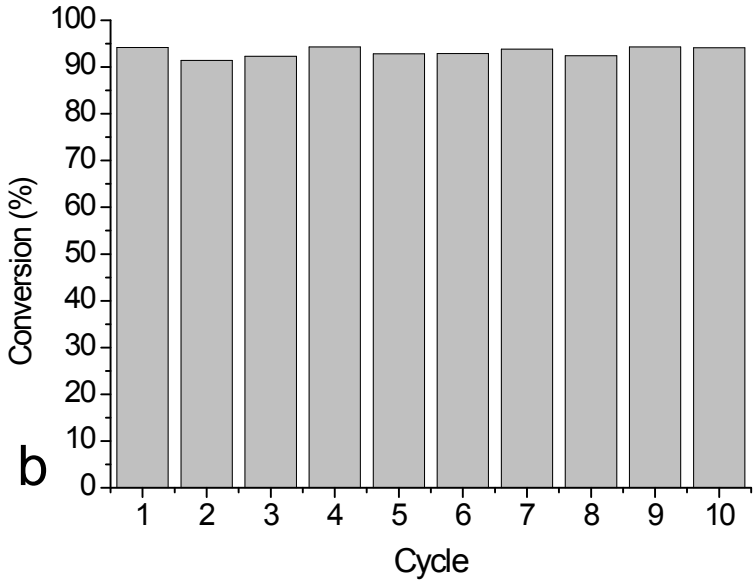

Fig. SI9. Conversion of benzylamine on Au/Ce_{60}-Ni_{10}-UVM-7(200) (a) and Au/Ce_{30}-Ni_{10}-UVM- 7(200) (b) catalysts over 10 successive cycles at 5 bar O_2 (115 ^{o}C, 4h, selectivity 100%).

.

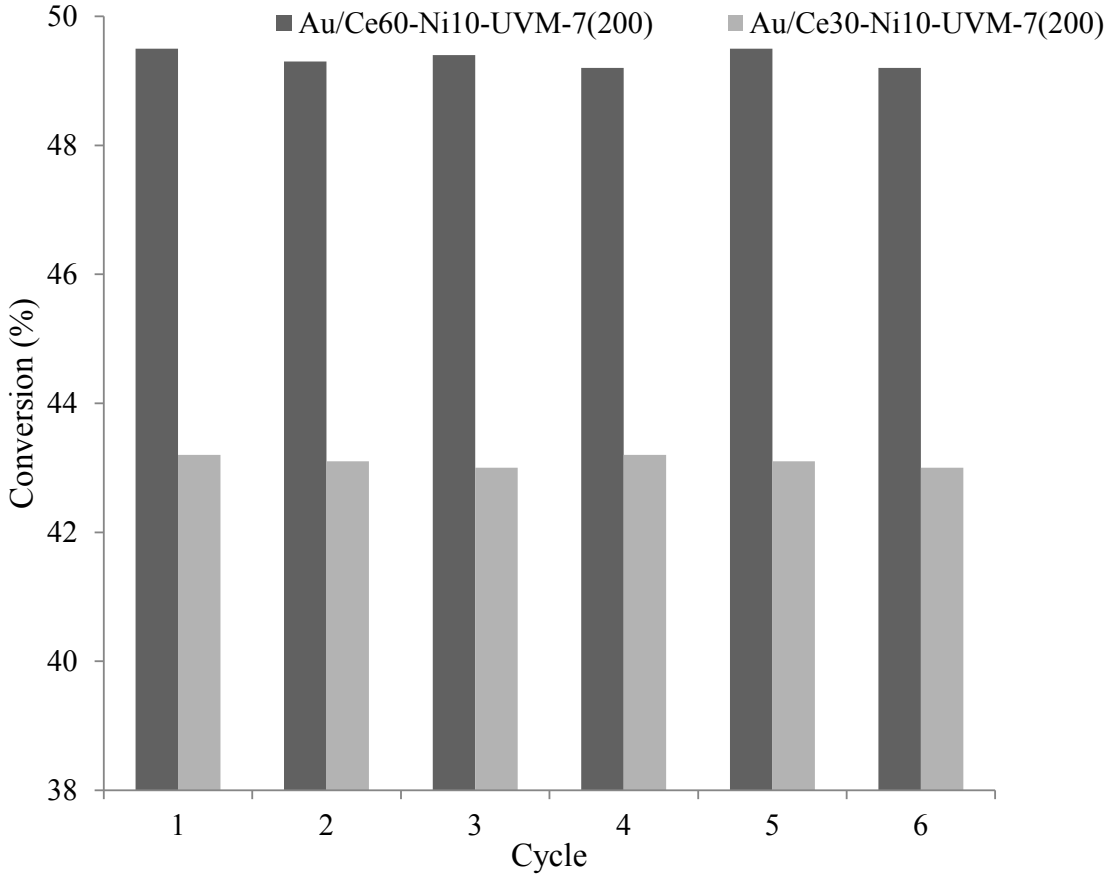

Fig. SI10. Conversion of benzylamine on Au/Ce_{60}-Ni_{10}-UVM-7(200) and Au/Ce_{30}-Ni_{10}-UVM- 7(200) catalysts over 6 successive cycles at 2 bar O_2 (115 ^{o}C, 4h, selectivity 100%).